

# Compressibility and High-Pressure Phase Transition of a Metalloporphyrin: (5,10,15,20-Tetraphenyl-21H,23H-porphinato)cobalt(II)

Robert M. Hazen,\* Thomas C. Hoering, and Anne M. Hofmeister

Geophysical Laboratory, Carnegie Institution of Washington, Washington, D.C. 20008

(Received: May 11, 1987)

Unit-cell parameters of the tetragonal metalloporphyrin, *meso*-(tetraphenylporphinato)cobalt(II), were determined at several pressures between 1 bar and 9 kbar, by using single-crystal X-ray diffraction techniques. Compression is uniform to about 5 kbar, with the *c* axis 3.4 times more compressible than *a*; *a* and *c* axis compressibilities are 1.47 (4) and 5.0 (2) (both  $\times 10^{-3}$  kbar<sup>-1</sup>), respectively. Bulk modulus  $K_0$  of this low-pressure phase is 108 (7) kbar, and  $K' = 7$  (4). At 4.9 (2) kbar the crystal transforms reversibly to a triclinic (pseudotetragonal) phase in which  $a = b$  and  $\gamma = 90^\circ$ , but cell angles  $\alpha$  and  $\beta$  deviate significantly from  $90^\circ$ . The axial compression ratio is 3.6, and *a* and *c* axis compressibilities are 2.0 (1) and 7.2 (2) (both  $\times 10^{-3}$  kbar<sup>-1</sup>), respectively. Zero-pressure bulk modulus of the high-pressure phase is 85 (12) kbar, and  $K' = 1$  (1). Thus, the high-pressure phase is significantly more compressible than the low-pressure phase. Infrared spectra were measured at several pressures to 141 kbar. Absorption bands broadened, decreased in intensity, and shifted at rates varying from  $-0.25$  to  $+1.3$  cm<sup>-1</sup> kbar<sup>-1</sup>. All but two of fifteen identifiable bands had positive shifts. No major discontinuities in the intensities or band positions occurred during compression. The observed crystallographic transformation is due predominantly to changes in intermolecular distances and configuration, with relatively little distortion of the intramolecular structure.

## Introduction

Hazen and Finger<sup>1</sup> recognized three principal compression mechanisms in solids: nearest neighbor bond compression, reduction of bond angles, and intermolecular compression. Bond compression and bond angle bending are well documented in numerous high-pressure structure studies of minerals and mineral-like compounds,<sup>2</sup> but little work has been done to elucidate compression or high-pressure structures of molecular crystals.

The metalloporphyrin (5,10,15,20-tetraphenyl-21H,23H-porphinato)cobalt(II), C<sub>44</sub>H<sub>28</sub>N<sub>4</sub>Co (here abbreviated CoTPP), is available in euohedral, stable crystals that are particularly well-suited for such high-pressure investigations. Its unit cell is relatively small ( $a = 15.05$  Å,  $c = 13.97$  Å,  $V = 3167$  Å<sup>3</sup>), its symmetry is high (tetragonal, space group *I42d*), and the presence of the relatively heavy element cobalt enhances the X-ray scattering efficiency of the crystals.

The original objectives of this study were to measure compressibility of CoTPP and to relate this compression to the molecular structure. During the course of the experiments a reversible phase transition was observed. A secondary objective, therefore, is to describe this new transition and to relate it to possible transitions in other molecular crystals.

Under the high-pressure conditions used in this study, only the space group and size of the unit cell could be measured by X-ray diffraction. Supplementary high-pressure studies of the CoTTP infrared spectra were conducted in order to learn of possible changes in molecular bond lengths and bond angles during compression.

## Experimental Section

**Specimen Description.** Euohedral  $100 \times 100 \times 40$  μm crystals of CoTPP were handpicked under a binocular microscope from synthetic material (Aldrich Chemical Co., Milwaukee, WI; catalog no. 25.219-0).

**Room-Pressure Unit-Cell Parameters.** A single crystal was mounted on a glass fiber for preliminary room-pressure X-ray study. Unit-cell parameters were determined from data collected on an automated four-circle diffractometer with monochromatized Mo K $\alpha$  radiation. Diffractometer angles were measured for 28 reflections, each of which was measured in eight equivalent positions.<sup>3,4</sup> Unit-cell parameters were refined initially as triclinic;

lattice parameters were found to conform to tetragonal dimensionality and final values were refined with tetragonal constraints (Tables I and II).

Swanson et al.<sup>5</sup> noted that systematic errors result in refined unit-cell parameters that differ, depending on the range of reflection  $2\theta$  used in the refinement. This phenomenon is evident in the present data. Reflections in the range from the  $9^\circ$  to  $13^\circ$   $2\theta$  result in a calculated cell volume of 3166.3 Å<sup>3</sup>; from  $12^\circ$  to  $15^\circ$  a volume of 3164.8 Å<sup>3</sup>; and from  $18^\circ$  to  $21^\circ$  a volume of 3162.5 Å<sup>3</sup> (Table I). Higher angle data thus yield significantly smaller unit-cell volumes. It is essential when results at different pressures are compared that the same range of  $2\theta$  be employed.

**High-Pressure Unit-Cell Parameters.** All high-pressure data were collected on a crystal of CoTPP mounted in a Merrill-Bassett type diamond-anvil cell.<sup>6,2</sup> Glycerin was employed as the hydrostatic pressure medium and several 5–10-μm diameter chips of ruby were added for pressure calibration.<sup>7</sup>

Lattice parameters at each pressure were refined from diffractometer angles of 10–14 reflections with  $2\theta < 14^\circ$ . Higher angle reflections would have been more desirable for lattice parameter measurements, but no reflections with  $2\theta > 14^\circ$  have sufficient intensity. Even the low-angle reflections employed in this study have an average intensity of only 40 count s<sup>-1</sup>, which is minimal for satisfactory peak centering.

All lattice parameters were refined initially as triclinic (Table I). Parameters for CoTPP up to 5.0 kbar conformed to tetragonal dimensionality and were also refined with tetragonal constraints (Table II).

**Infrared Spectra.** Spectra were measured in a diamond-anvil cell similar to that described by Mao and Bell.<sup>8</sup> A Nicolet 7199 Fourier transform infrared optical bench equipped with a liquid nitrogen cooled mercury cadmium telluride detector for the mid-IR and a liquid helium cooled bolometer (Model HD-3; Infrared Laboratories Inc., Tucson, AZ) for the far-IR were employed. A Nicolet 1280 data processing unit was used for spectral acquisition. An all-reflecting 4 $\times$  beam condenser was used as described by Hofmeister et al. (in press).

Pressures were gauged by the shift of the R1 fluorescence line of ruby powder covering the sample. Small crystals of the porphyrin were placed in the diamond-anvil cell and squeezed to form

(1) Hazen, R. M.; Finger, L. W. *Sci. Am.* **1985**, *252*, 110–117.

(2) Hazen, R. M.; Finger, L. W. *Comparative Crystal Chemistry*; Wiley: New York, 1982.

(3) Hamilton, W. C. *International Tables for X-ray Crystallography*; Kynock: Birmingham, 1984; Vol. 4, pp 273–284.

(4) King, H. E.; Finger, L. W. *J. Appl. Crystallogr.* **1979**, *12*, 374–378.

(5) Swanson, D. K.; Weidner, D. J.; Prewitt, C. T.; Kandelin, J. J. *EOS, Trans. Am. Geophys. Union* **1985**, *66*, 370.

(6) Merrill, L.; Bassett, W. A. *Rev. Sci. Instrum.* **1974**, *45*, 290–294.

(7) Barnett, J. D.; Block, S.; Piermarini, G. J. *Rev. Sci. Instrum.* **1973**, *44*, 1–9.

(8) Mao, H. K.; Bell, P. M. *Year Book Carnegie Inst. Washington* **1978**, *77*, 904–913.

**TABLE I: Unit-Cell Parameters of *meso*-(Tetraphenylporphinato)cobalt(II) Refined as Pseudotetragonal without Symmetry Constraints (i.e., as Triclinic); 9–13° Data Unless Otherwise Noted**

press., kbar	<i>a</i> , Å	<i>b</i> , Å	<i>c</i> , Å	$\alpha$ , deg	$\beta$ , deg	$\gamma$ , deg	<i>V</i> , Å <sup>3</sup>	<i>V</i> / <i>V</i> <sub>0</sub>
0.001 <sup>a</sup>	15.048 (7) <sup>b</sup>	15.058 (4)	13.974 (9)	89.97 (4)	90.00 (5)	89.99 (3)	3166.3 (27)	1.000
0.001 <sup>c</sup>	15.062 (4)	15.055 (4)	13.957 (2)	89.99 (2)	90.01 (2)	90.02 (2)	3164.8 (13)	1.000
0.001 <sup>d</sup>	15.053 (3)	15.053 (3)	13.957 (2)	90.02 (1)	90.01 (1)	90.00 (2)	3162.5 (10)	0.999
~0.1 <sup>e</sup>	15.039 (9)	15.076 (7)	13.972 (11)	89.93 (7)	90.11 (6)	90.07 (5)	3167.9 (35)	1.001
2.1	15.005 (6)	15.009 (6)	13.817 (7)	90.04 (6)	90.00 (4)	89.99 (4)	3111.5 (25)	0.983
2.9	14.988 (4)	14.990 (3)	13.753 (5)	90.02 (3)	90.02 (3)	90.02 (2)	3089.5 (15)	0.976
4.2	14.957 (4)	14.964 (3)	13.667 (5)	89.99 (3)	90.00 (3)	90.00 (2)	3058.8 (14)	0.966
4.8	14.950 (4)	14.953 (4)	13.634 (7)	89.99 (4)	90.02 (4)	90.04 (3)	3047.8 (21)	0.963
5.0	14.943 (6)	14.943 (6)	13.604 (9)	89.97 (6)	89.84 (4)	89.97 (4)	3037.6 (26)	0.959
5.2	14.944 (7)	14.940 (4)	13.581 (10)	90.37 (4)	89.78 (5)	89.99 (3)	3032.0 (27)	0.958
5.3	14.937 (5)	14.931 (3)	13.585 (7)	90.54 (3)	89.64 (4)	89.98 (2)	3029.5 (20)	0.957
5.8	14.945 (6)	14.897 (4)	13.523 (10)	90.69 (4)	89.55 (4)	89.88 (3)	3010.3 (23)	0.951
5.9	14.920 (7)	14.916 (3)	13.523 (10)	90.32 (4)	89.58 (5)	89.95 (3)	3009.3 (28)	0.950
7.1	14.875 (4)	14.879 (2)	13.403 (7)	90.27 (3)	89.17 (3)	89.99 (2)	2966.1 (19)	0.937
8.0	14.887 (8)	14.860 (4)	13.293 (9)	90.00 (4)	88.84 (5)	90.15 (3)	2940.3 (28)	0.929
9.0	14.832 (11)	14.839 (7)	13.208 (12)	90.64 (6)	88.31 (7)	90.01 (5)	2905.4 (38)	0.918

<sup>a</sup>Crystal in air; 9–13° data. <sup>b</sup>Parenthesized figures represent esd's. <sup>c</sup>Crystal in air; 12–15° data. <sup>d</sup>Crystal in air; 18–21° data. <sup>e</sup>Crystal in cell with air bubble.

**TABLE II: Unit-Cell Parameters of *meso*-(Tetraphenylporphinato)cobalt(II) with Tetragonal Symmetry Constraints<sup>a</sup>**

press., kbar	<i>a</i> , Å	<i>c</i> , Å	<i>V</i> , Å <sup>3</sup>	<i>V</i> / <i>V</i> <sub>0</sub>	<i>c</i> / <i>a</i>
0.001	15.055 (3) <sup>b</sup>	13.972 (9)	3167.0 (24)	1.000	0.9281
0.1	15.062 (6)	13.938 (16)	3161.9 (39)	0.998	0.9254
2.1	15.007 (4)	13.816 (9)	3111.6 (24)	0.983	0.9206
2.9	14.989 (2)	13.750 (6)	3089.0 (14)	0.975	0.9173
4.2	14.962 (2)	13.664 (6)	3058.6 (14)	0.966	0.9132
4.8	14.951 (3)	13.630 (8)	3046.9 (19)	0.962	0.9116
5.0 <sup>c</sup>	14.947 (4)	13.621 (11)	3043.3 (28)	0.961	0.9113

<sup>a</sup>All unit-cell parameters are based on least-squares refinement of from 8 to 14 reflections for which  $2\theta < 14^\circ$ . <sup>b</sup>Parenthesized figures represent esd's. <sup>c</sup>The 5.0-kbar unit cell deviates significantly from tetragonal symmetry (see Table I;  $\beta = 89.84 \pm 0.04^\circ$ ).

a film with a thickness appropriate to absorbance measurements. CsI was used as the pressure medium for the mid-IR, but no pressure transmission medium was used for the far-IR.

It is not possible to maintain pressures below about 25 kbar with the lever-arm design of the diamond-anvil cell used in infrared experiments.<sup>8</sup> Spectra were initially measured, therefore, at a minimum pressure of 25 kbar, after which spectra at increasing then decreasing pressure were obtained.

## Results

**Compression from 1 bar to 5 kbar.** Lattice parameters and unit-cell volume vary smoothly as a function of pressure below 5 kbar. Tetragonal unit-cell edges as a function of pressure and average compressibilities (1 bar to 5 kbar) are

$$a = 15.057 (2) - [0.025 (2)]P + [0.0007 (3)]P^2 \quad (1)$$

$$\beta_a = 0.00147 (4) \text{ kbar}^{-1} \quad (2)$$

$$c = 13.967 (7) - [0.080 (6)]P + [0.002 (1)]P^2 \quad (3)$$

$$\beta_c = 0.0050 (2) \text{ kbar}^{-1} \quad (4)$$

The *c* axis is 3.4 times more compressible than *a* (Figure 1), resulting in a steadily decreasing *c/a* with increasing pressure (Table I). Both axes display significant curvature as reflected in the second-order terms in eq 1 and 3.

A least-squares fit of unit-cell volume as a function of pressure to a Birch–Murnaghan equation of state

$$P = 1.5K_0[(V_0/V)^{7/3} - (V_0/V)^{5/3}] \times [1 - 0.75(4 - K')][(V_0/V)^{2/3} - 1] \quad (5)$$

yields a bulk modulus  $K_0 = 108 (7) \text{ kbar}$  and  $K' = 7 (4)$ , with initial volume  $V_0 = 3167 \text{ Å}^3$ .

**The High-Pressure Phase.** At 5 kbar and higher pressures the unit-cell parameters deviate significantly from tetragonal di-

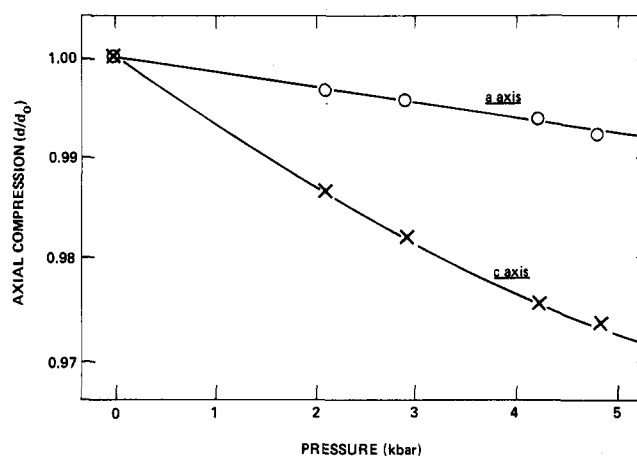


**Figure 1.** Relative cell-edge compression ( $d/d_0$ ) for CoTPP vs. pressure. The *c* axis is 3.4 times as compressible as *a*.

mensionality. Both  $\alpha$  and  $\beta$  unit-cell angles diverge from  $90^\circ$  at 4.9 (2) kbar, thus indicating a distortional phase transition from tetragonal to lower symmetry (Figure 2). At first it was thought that the high-pressure phase was monoclinic, a symmetry consistent with the conditions  $a = b$  and  $\alpha = (180 - \beta)$ . For example, the pseudotetragonal unit-cell parameters at 5.3 kbar are  $a \approx b = 14.93 \text{ Å}$  and  $c = 13.59 \text{ Å}$ ;  $\alpha \approx (180 - \beta) = 90.5^\circ$  and  $\gamma = 90^\circ$ . The equivalent monoclinic unit cell is end-centered with  $\alpha \approx \beta = 21.1 \text{ Å}$  and  $c = 13.57 \text{ Å}$ ;  $\alpha = \gamma = 90^\circ$  and  $\beta = 90.7^\circ$ . It is evident from Figure 2, however, that  $\alpha$  and  $\beta$  do not vary sympathetically, except perhaps between 5 and 6 kbar. The  $\beta$  angle decreases linearly with pressure, whereas  $\alpha$  appears to increase initially and then maintain a value slightly greater than  $90^\circ$ .

The transition is rapid and completely reversible; data in Table I (illustrated on Figure 2) include four cycles between the low- and high-pressure phases. There is no apparent volume discontinuity ( $\Delta V < 0.05\%$ ) at the 4.9-kbar transition. The phase change is thus consistent with a second-order transformation. It is significant that, in spite of the phase transition, the (001) plane retains its 4-fold dimensional symmetry. At all pressures  $a = b$  and  $\gamma = 90^\circ$  within the error of measurement. These conditions are not related to any symmetry operators of the observed triclinic space group.

Average axial compressibilities between 5 and 9 kbar are greater than at lower pressure:

$$\beta_a \approx \beta_b = 0.0020 (1) \text{ kbar}^{-1} \quad (6)$$

$$\beta_c = 0.0072 (2) \text{ kbar}^{-1} \quad (7)$$

The *c* axis of 3.6 times more compressible than *a*, which is comparable to the 3.4 compression ratio below the transition.

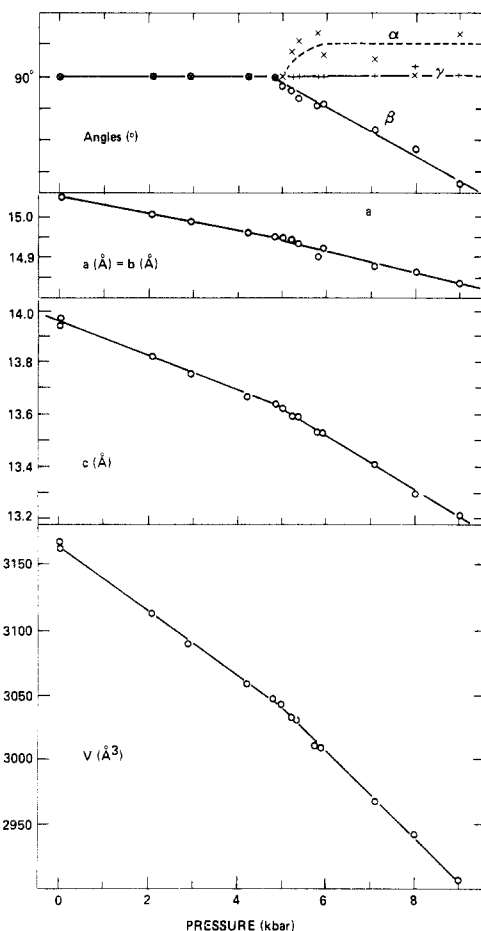


**Figure 2.** Unit-cell parameters and volume of CoTPP vs. pressure. Average unit-cell errors are smaller than the data symbols. A distortional phase transition from tetragonal to triclinic dimensional symmetry occurs at  $4.9 \pm 0.2$  kbar.

Equation-of-state parameters for the high-pressure phase were calculated from eight pressure–volume points (Table I). Zero-pressure bulk modulus is 85 (12) kbar, with  $K' = 1$  (1). Thus, the high-pressure CoTPP is significantly more compressible than the low-pressure phase.

**Infrared Spectra to 141 kbar.** Normal coordinate analysis of tetraethyl metalloporphyrins substituted by various metals has been carried out by Ogoshi et al.<sup>9</sup> Many of their vibrational assignments could be correlated for the tetraphenyl compound used in this study. Vibrations due to the peripheral phenyl groups could be identified as well. The peak positions of all bands except two increase slightly with pressure. The magnitude of the positive pressure shift is, to a first approximation, correlated with band assignments. Bands near 3000  $\text{cm}^{-1}$  attributed to C–H stretching have the greatest slopes of about  $1 \text{ cm}^{-1} \text{ kbar}^{-1}$ . The far-IR bands associated with ring deformations and metal–nitrogen stretching motions have modest slopes of about  $0.7 \text{ cm}^{-1} \text{ kbar}^{-1}$ . The majority of bands associated with the phenyl groups and the porphine ring (for example, the ring-deformation band at a frequency of about  $1000 \text{ cm}^{-1}$ ; Table III) had smaller slopes between  $0.2$  and  $0.5 \text{ cm}^{-1} \text{ kbar}^{-1}$  although a few values ranged from 0 to  $0.7 \text{ cm}^{-1} \text{ kbar}^{-1}$ .

The slight negative pressure shift of the band at  $900 \text{ cm}^{-1}$  associated with ring deformation indicates that the distortion from the low-pressure to high-pressure is altering the bonding within the ring. A moderate negative pressure shift of an unassigned  $1800\text{-cm}^{-1}$  feature indicates that this band is a fundamental, because no bands of lower energy can combine to give the correct frequency and pressure derivative.

Certain high-frequency bands, such as the ones at  $3035$  and  $3070 \text{ cm}^{-1}$ , due respectively to C–H in-plane vibrations of the

**TABLE III: Changes in Selected Infrared Absorption Maxima of CoTPP with Increasing Pressure**

press., kbar	$\nu$ , $\text{cm}^{-1}$	press., kbar	$\nu$ , $\text{cm}^{-1}$
Absorption Maxima of "Quadrant Stretching" of Phenyl Groups			
0	1600	23	1612
6.4	1603	40	1619
12	1605	69	1632
Absorption Maxima of In-Plane Ring-Deformation Frequencies of the Porphine Ring			
0	1007	40	1018
4.7	1007	47	1016
6.4	1009	69	1020
12	1011	100	1019
23	1015	141	1028

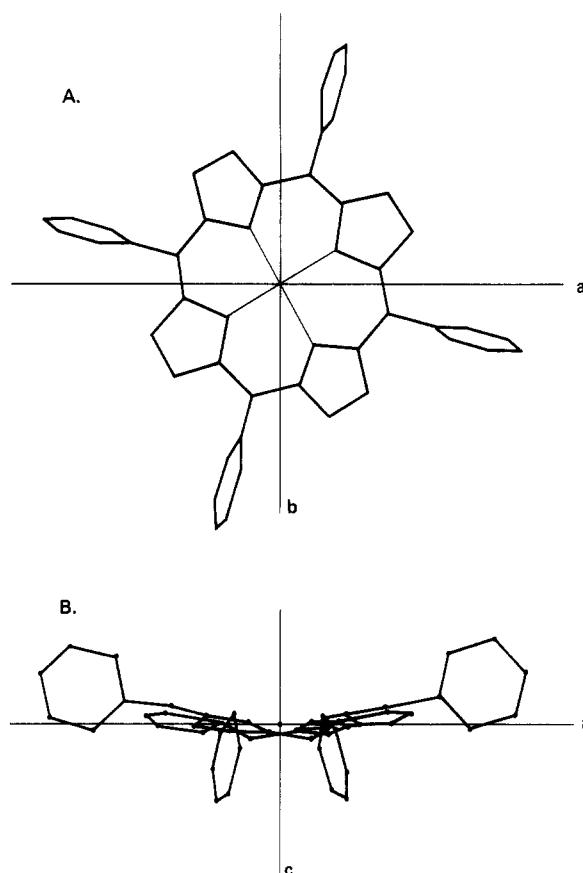


**Figure 3.** CoTPP molecule, consisting of four interconnected pyrrole rings in planar conformation with four benzene rings in a paddlewheel orientation.

porphine ring and C–H vibrations of the phenyl groups, have a pronounced broadening with increasing pressure. This effect is enhanced over that for lower frequency bands and practically obliterates the high-frequency components above 20 kbar. This observation argues that pressure gradients across the sample are not the sole cause of spectral broadening.

### Discussion

**Structural Inferences: The Low-Pressure Phase.** The structure of CoTPP was elucidated by Madura and Scheidt.<sup>10</sup> Stevens<sup>11</sup> subsequently presented detailed crystal structure information, including high-resolution electron density distribution. The CoTPP molecule consists of a planar grouping of four interconnected pyrrole rings, with four branching benzene rings in a "paddlewheel" orientation (Figure 3). The crystal structure consists of a body-centered tetragonal array of these CoTPP molecules, each of which has 4 point symmetry (Figure 4).

(9) Ogoshi, H.; Saito, Y.; Nakamoto, K. *J. Chem. Phys.* **1972**, *57*, 4194–4202.

(10) Madura, P.; Scheidt, W. R. *Inorg. Chem.* **1976**, *15*, 3182–3185.

(11) Stevens, E. D. *J. Am. Chem. Soc.* **1981**, *103*, 5087–5095.

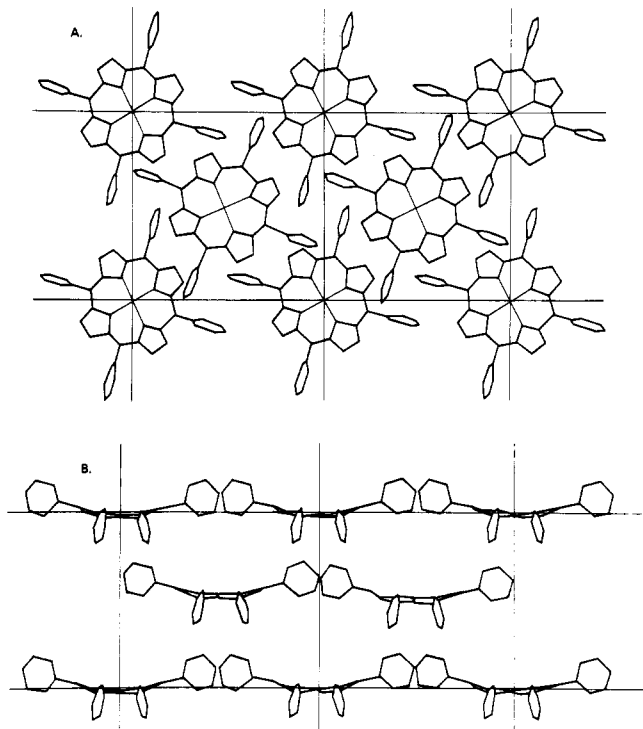


**Figure 4.** Structure of CoTPP, after Stevens.<sup>9</sup> (A) A (001) projection shows how CoTPP molecules occupy lattice points of a body-centered tetragonal unit cell. Six molecules at the corners lie at  $z = 0$ , whereas the two centered molecules are at  $z = 1/2$ . (B) A (100) projection reveals how the CoTPP molecules lie in the (001) planes. Intermolecular distances are greater between molecules parallel to  $c$  than in the (001) plane.

Complete three-dimensional structure refinements of CoTPP at high pressure were precluded by the weak intensities of diffraction maxima. Several lines of evidence, however, lead to the inference that almost all compression of CoTPP is intermolecular. First, the anisotropy of compression, with  $c$  3.4 times more compressible than  $a$ , reflects the planar aspect of the molecules. Intermolecular regions constitute most of the distance parallel to  $c$  but only about a fourth of the distance parallel to  $a$ . Second, the magnitude of axial compression, on the order of  $0.005 \text{ kbar}^{-1}$  parallel to  $c$ , is typical of intermolecular compression in graphite, boron nitride, and  $\text{SnS}_2$ .<sup>12</sup> Axial compressibilities greater than  $0.001 \text{ kbar}^{-1}$  are uncommon in compounds with no intermolecular bonds. Third, the significant curvature of axial length vs. pressure plots (Figure 1) and the large  $K'$  of 7 are characteristic of intermolecular compression. Forces controlling intermolecular compression differ from forces controlling cation-anion-type bonding characteristic of most minerals, for which  $K'$  is typically 4.

**Structural Inferences: The High-Pressure Phase.** Structural aspects of the high-pressure phase may be inferred, in part, from two notable properties of CoTPP above 5 kbar. First, this high-pressure phase is more compressible than the topologically

related low-pressure phase. This seemingly paradoxical behavior is typical of reversible phase transitions in which the high-pressure phase has more "compressional degrees of freedom" than the low-pressure phase. Rhenium trioxide,  $\text{ReO}_3$ , is one of the most dramatic examples of this phenomenon.<sup>13,14</sup> At low pressure the compound is cubic and Re-O bond compression is the only compression mechanism; the bulk modulus is greater than 2 Mbar. At about 5 kbar the oxide transforms reversibly to a lower symmetry form in which bending of Re-O-Re angles is added as a compression mechanism; the bulk modulus drops to about 200 kbar. The high-pressure phase is an order of magnitude more compressible than the low-pressure phase because distortion to a lower symmetry introduces a new compression mechanism. The same situation appears to obtain in CoTPP. Intermolecular compression at low pressure conforms to the tetragonal symmetry constraints. The benzene rings lie above molecules in adjacent layers, while molecules in alternate layers exactly superimpose. Above 5 kbar no such constraints obtain, and molecules may adopt more staggered superpositions.

Of special note is the 4-fold dimensional symmetry of (001) planes in the high-pressure phase. It might at first appear that each layer of the structure, and by inference each molecule that composes the layer, retains the symmetry of the low-pressure phase. However, in spite of the retention of a dimensionally square net, the  $a$  and  $b$  axes are significantly more compressible in the high-pressure phase than in the low-pressure phase. It would seem, therefore, that some subtle, but important, structural change has occurred within, as well as between, the layers, even though this change produces no obvious effects on the infrared spectra.

#### Conclusions

The behavior of CoTPP may be representative of many other high-symmetry molecular solids at high pressure. Intermolecular bonds typically compress by  $0.005 \text{ kbar}^{-1}$ , resulting in large volume changes at relatively low pressures. Crystals composed of small molecules (with a correspondingly large intermolecular volume) are thus expected to have bulk moduli on the order of 100 kbar. Most constituent molecules, on the other hand, should be fairly rigid. If molecular conformation does not change significantly, then intramolecular compression will contribute little to the crystal's pressure-volume response, a conjecture that is borne out by the infrared studies.

Distortional phase transitions, in which the arrangement of rigid molecules is slightly altered, may be an energetically favorable mode of compression in many organometallics. An increase in the number of compressional degrees of freedom may result from a decrease in symmetry; high-pressure phases of molecular solids, consequently, may commonly display greater compressibility than their low-pressure counterparts.

**Acknowledgment.** We thank Charles T. Prewitt for his constructive review of the manuscript. This research was supported in part by National Science Foundation Grant EAR84-19982 and by the Carnegie Institution of Washington.

**Registry No.** CoTPP, 14172-90-8.

(13) Schirber, J. E.; Morosin, B. *Phys. Rev. Lett.* **1979**, *42*, 1485-1487.

(14) Schirber, J. E.; Morosin, B.; Alkire, R. W.; Lawson, A. C.; Vergamini, P. J. *Phys. Rev. B: Condens. Matter* **1984**, *29*, 4150-4152.

(12) Hazen, R. M.; Finger, L. W. *Am. Mineral.* **1978**, *63*, 289-292.